

How is sensory information processed?

Ilya Nemenman

Kavli Institute for Theoretical Physics
University of California,
Santa Barbara, California 93106

November 16, 2018

Abstract

Advances in statistical learning theory leave us with many possible designs of learning machines. But which of them are implemented by brains, metabolic and genetic networks, and other biological information processors? We analyze how various abstract Bayesian learners would perform on different data, including natural ensembles, and discuss possible experiments that can determine which learning-theoretic computation is performed by a particular organism.

1 Introduction

There is a lot of similarities between metabolic, genetic, and neuronal networks. They measure their environment, process the measured information, make estimations of the quantities of interest, and responds appropriately. In other words, in the sense of the theory of statistical inference (Vapnik, 1998), all of these are *learning machines* that have functional differences mainly with respect to the statistics of the input signals and the repertoires and time scales of responses. Therefore, one might expect that all these systems are trying to (efficiently) implement similar abstract learning-theoretic computations, be that extraction and efficient representation of the sensory information (Attneave, 1954; Barlow, 1959, 1961; Atick, 1992), or of its part that is relevant to making predictions about the world (Bialek et al., 2001), or something else. But which exact computations are being performed? What is, for example, a Bayesian learning-theoretic model equivalent to a rat (Gallistel et al., 2001) or a simple neuronal network (Seung, 2003) that tries to maximize its reward?

To answer this, one could construct a biologically plausible computing network that is able to perform computations needed by a particular learning machine (Rao, 2004) and then search for real biological systems that look similar. Another approach is not to model the biological computation but to see which of the abstract learners responds to different input signals in the same way as a real creature under consideration. To follow this route, one needs to understand various model machines fairly well. Thus this paper consists of two parts. We start by investigating Bayesian statistical inference by different learners, paying particular attention to two *complete* ones, both of which can solve an arbitrary

complex learning problem (Secs. 2 through 6). Discussion of how our new knowledge can be used to uncover a learning–theoretic equivalent behind a particular biological system constitutes the second part of the paper (most of Secs. 7 and 8). However, searching for connections between abstract learning setups and the biological machinery capable of implementing them remains out of our scope.

An important point helps us to compare the two complete learning machines. Properties of learning depend on the ensemble of possible input signals (Vapnik, 1998; Bialek et al., 2001), and natural ensembles have particular traits that persist for biological systems of very different origins. Consider the biochemical network that is responsible for transforming the number of photons hitting a photoreceptor into an estimate of the instantaneous light intensity (Detwiler et al., 2000). This estimate depends on the details of the network, which embody the a priori expectations that the network has about the probability distribution of intensities in some not yet understood way. In principle, any such distribution can be realized. However, in practice, instantaneous intensity is determined by the statistics of reflectivities of objects that come in the view and by the mean ambient light intensity. The statistics barely change over long time scales, while the mean intensity depends on, for example, clouds shading the sun and varies rapidly. The network may want to learn intricate details of the distribution of reflectivities to make its estimates, but before that it should get very accurate and fast at learning the mean light level, as this is the most and the fastest varying unknown. A similar separation of time scales is observed in genetic regulatory networks, where, for example, changes in the lactose concentration happen on the scale of minutes, while statistics of lactose bursts depends on the environment and is constant for generations. In neuroscience, when estimating its angular velocity, a fly takes into the account the preceding velocity variance, and it may or may not have time for and be reacting to higher order moments (Fairhall et al., 2002). It turns out that the learning machines we consider assign “importance” to various dimensions of the complex inputs differently, and this lets us distinguish them by studying responses to natural stimuli.

Most of our analysis is abstract and is built upon usual learning–theoretic constructions. Thus the results of the first part of the paper have value beyond biological applications, which were the original motivation for this work. Because of the heavy emphasis on the abstract description, some ideas presented here have appeared in the previous literature. However, to elucidate important points that might have been of a lesser interest in other contexts, we make this presentation complete and reasonably self-contained. Further, since our observations are often simple extensions of earlier results, wherever a strict mathematical derivation could be replaced by an intuitive qualitative argument, we chose clarity over rigor. An interested reader will find it easy to fill in all the missing details.

2 The basics of learning

Learning machines should be powerful enough to explain complex phenomena. However, when data is scarce this power leads to overfitting and poor generalization. Thus a balance must be struck between the abilities to explain and to overfit, and this balance will depend on the amount of data available. In accord, much of statistical learning theory (Jefreys, 1936; Schwartz, 1978; Janes, 1979; Rissanen, 1989; Clarke and Barron, 1990; MacKay,

1992; Balasubramanian, 1997; Vapnik, 1998; Nemenman, 2000; Bialek et al., 2001) has been devoted to putting the famous paradigm of William of Ockham, *Pluralitas non est ponenda sine neccesitate*, on firm mathematical footing in various theoretical frameworks. In particular, in Bayesian formulation (Press, 1989), we know now how proper Bayesian averaging creates *Occam factors* that punish for complexity and weigh posterior probabilities towards those estimates among a *finite* set of *parametric* model families that have the best overall predictive power (Bialek et al., 2001), but do not necessarily produce the best fit to the observed data. This has been called *Bayesian model selection*.¹

The waters get murkier in a *nonparametric* or *infinite parameter* setting when the whole functional form of an unknown object is to be inferred. Bayesian nonparametric developments generally parallel parametric ones, and techniques of Quantum Field Theory (QFT) help in computations (Bialek et al., 1996; Holy, 1997; Bialek et al., 2001; Cucker and Smale, 2001; Nemenman and Bialek, 2002). However, the exact relationship between the two settings is unknown, and some results suggest subtle logarithmic differences between the cases (Hall and Hannan, 1988; Rissanen et al., 1992; Bialek et al., 2001).

We will analyze these and other learning machines in Bayesian context, and we start with an introduction of some important useful quantities.

Suppose we observe i. i. d. samples $x_i, i = 1 \dots N$. For simplicity we assume that x is a scalar, but this does not affect most of the discussion. We need to estimate the probability density that generates the samples. A priori we know that this density, $Q(x|\alpha)$, can be indexed by some (possibly infinite dimensional) vector of parameters α , and the probability of each parameter value is $\mathcal{P}(\alpha)$. We can define the *density of models (solutions)*, at a given *distance (dissimilarity, or divergence)* $D(\bar{\alpha}, \alpha) = \epsilon$ away from the unknown true target $\bar{\alpha}$, which we are trying to learn:

$$\rho(\epsilon; \bar{\alpha}) = \int d\alpha \mathcal{P}(\alpha) \delta [D(\bar{\alpha}, \alpha) - \epsilon] . \quad (1)$$

For Bayesian inference of probability densities, the correct measure of dissimilarity is the Kullback–Leibler divergence, $D_{\text{KL}}(\bar{\alpha}||\alpha) = \int dx Q(x|\bar{\alpha}) \log[Q(x|\bar{\alpha})/Q(x|\alpha)]$ (Bialek et al., 2001), which has an important information–theoretic interpretation (Cover and Thomas, 1991). However, in other situations different choices of D can and should be made.

Performance of a Bayesian learner is usually measured by the speed with which the posterior probability concentrates for $N \rightarrow \infty$ (the *learning curve*) and by whether the point of concentration is the true unknown target (*consistency*). These characteristics illuminate the importance of ρ , as it relates to both of them. First, it has been proven that if for $\epsilon \rightarrow 0$ the density, $\rho(\epsilon; \bar{\alpha})$, is not identically zero, then the Bayesian problem is consistent (Nemenman, 2000; Bialek et al., 2001). Intuitively, this is because, for large density, statistical fluctuations of the samples and of the estimated parameters will result in small $D_{\text{KL}}(\bar{\alpha}||\text{estimate})$, making convergence to the target almost certain.

Relation of ρ to the learning curve is more complicated. We can calculate the average (over samples) Occam factor for a given target (the *generalization error*, or the *fluctuation*

¹With the creationism–evolution tension mounting in teaching of biology in the U. S. schools, it is amusing to see how two friars, William of Ockham and Thomas Bayes, teamed up with modern day mathematicians to produce, in my view, the clearest formulation of the theory of learning from past experiences. If this approach results in a better understanding of biological designs, the situation will be even more peculiar.

determinant) to the leading order in $1/N$:

$$\mathcal{D}(\bar{\alpha}; N) = -\log \int d\epsilon \rho(\epsilon; \bar{\alpha}) e^{-N\epsilon}. \quad (2)$$

This is the term that emerges as the penalty for complexity in Bayesian model selection, as we will see later. If averaged over $\bar{\alpha}$, the Occam factor results in *predictive information* (Bialek et al., 2001), which is the number of bits the past N samples provide about all of the future:

$$I_{\text{pred}}(N) = \int d\bar{\alpha} \mathcal{P}(\bar{\alpha}) \mathcal{D}(\bar{\alpha}; N). \quad (3)$$

Finally, one can define the *universal learning curve*, which measures the expected D_{KL} between the target and the estimate after N observations (Bialek et al., 2001):

$$\Lambda(\bar{\alpha}; N) = \frac{d\mathcal{D}(\bar{\alpha}; N)}{dN}, \quad (4)$$

$$\Lambda(N) = \int d\bar{\alpha} \mathcal{P}(\bar{\alpha}) \Lambda(\bar{\alpha}; N) = \frac{dI_{\text{pred}}}{dN}. \quad (5)$$

As an example, consider a setup where α can take M discrete values a_1, a_2, \dots, a_M with a priori probabilities $\mathcal{P}_1, \mathcal{P}_2, \dots, \mathcal{P}_M$, and their divergences from the target a_1 are $0 = d_1 < d_2 < \dots < d_M$. The density is $\rho(\epsilon; a_1) = \sum_{i=1}^M \mathcal{P}_i \delta(d_i - \epsilon)$. For $N \rightarrow \infty$ this gives

$$\mathcal{D}(a_1; N) = -\log \sum_{i=1}^M \mathcal{P}_i \exp[-Nd_i] \approx -\log \mathcal{P}_1 - \mathcal{P}_2/\mathcal{P}_1 \exp[-Nd_2], \quad (6)$$

$$\Lambda(a_1; N) \approx d_2 \mathcal{P}_2/\mathcal{P}_1 \exp[-Nd_2]. \quad (7)$$

So exponential learning curves (and asymptotically finite \mathcal{D} and I_{pred}) correspond to learning a possibility in a finite set. Similarly, we can construct models with $\Lambda(N) \propto 1/N^\nu$, $\nu > 1$, and they will also have asymptotically finite I_{pred} . Cases of divergent predictive information² and slower decaying learning curves are discussed in the next sections.

3 (Not quite) finite parameter learning

Suppose the target, that is the unknown probability density $\bar{Q}(x)$ that generates the observations, belongs to one of R sets of densities, the *model families*, A_r , $r = 1 \dots R$, with $\text{Prob}(\bar{Q} \in A_r) = \mathcal{P}(r)$. Distributions, or *models*, in each of the families are indexed by parameters $\alpha^{(r)}$, $\dim \alpha^{(r)} = K(r) < \infty$, so that the density of observing x in a given model is $Q_r(x|\alpha^{(r)})$. Since the data are independent, $Q_r(\{x\}|\alpha) = \prod_{i=1}^N Q_r(x_i|\alpha^{(r)})$. Within each family, the parameters are a priori distributed according to $\mathcal{P}(\alpha^{(r)}|r)$.

We will assume that the families are *nested*. By this we mean that $Q_r(x|\alpha^{(r)}) \equiv Q(x|\alpha)$ are independent of r , but that in each family the values of α_μ , $\mu > K(r)$, are identically

²Significance of this divergence and its connections to definitions of complexity were analyzed by Bialek et al. (2001).

zero. Further, the nonzero parameters have the same a priori distributions in all families:

$$\mathcal{P}(\alpha_\mu|r) = \begin{cases} p(\alpha_\mu), & \mu \leq K(r) \\ \delta(\alpha_\mu), & \mu > K(r) \end{cases} \quad (8)$$

$$\mathcal{P}(\boldsymbol{\alpha}|r) = \prod_{\mu=1}^R \mathcal{P}(\alpha_\mu|r) \quad (9)$$

Thus a parameter α_μ is “switched on” when r reaches $r_\mu \equiv \min_r \{r : K(r) \geq \mu\}$.

If $R \rightarrow \infty$, then we require that the union of all families forms a *complete* set, so that every sufficiently smooth probability density can be approximated arbitrarily closely by some member of the union (if needed, this definition can be made more precise).

For simplicity, in this paper we will focus on the case³

$$p(\alpha_\mu) = \mathcal{N}(0, \sigma_\mu^2), \quad (10)$$

$$\sigma_\mu = c r_\mu^{-\beta}, \quad \beta \geq 0, \quad c = \text{const}, \quad (11)$$

where $\mathcal{N}(a, b)$ denotes a normal distribution with the mean of a and the variance of b . In particular, $\beta = 0$ corresponds to the same in-family a priori variances for all nonzero parameters. This is common when discussing Bayesian model selection.

While the priors describe a set of parametric models, another view is also possible. The joint distribution of r , $\boldsymbol{\alpha}$, and $\{x\}$ is $P(\{x\}, \boldsymbol{\alpha}, r) = Q(\{x\}|\boldsymbol{\alpha})\mathcal{P}(\boldsymbol{\alpha}|r)\mathcal{P}(r)$, which results in

$$\begin{aligned} P(\{x\}, \boldsymbol{\alpha}) &= \sum_r Q(\{x\}|\boldsymbol{\alpha})\mathcal{P}(\boldsymbol{\alpha}|r)\mathcal{P}(r) = Q(\{x\}|\boldsymbol{\alpha}) \sum_r \mathcal{P}(\boldsymbol{\alpha}|r)\mathcal{P}(r) \\ &\equiv Q(\{x\}|\boldsymbol{\alpha})\mathcal{P}(\boldsymbol{\alpha}), \end{aligned} \quad (12)$$

where the last equation defines $\mathcal{P}(\boldsymbol{\alpha})$, the overall prior over $\boldsymbol{\alpha}$. Unlike $\mathcal{P}(\boldsymbol{\alpha}|r)$, $\mathcal{P}(\boldsymbol{\alpha})$ is not factorizable and is not differentiable at zero for any α_μ , $\mu > K(1)$. Thus the nested setup may be viewed as the inference in a combined model family with $K(R)$ parameters. In particular, for R and $K(R) \rightarrow \infty$, the learning problem has a countable infinity of parameters leading to the common assumption of equivalence with the nonparametric inference.

It is of interest to calculate the combined a priori mean and variance of $\boldsymbol{\alpha}$. Integrating over all α_ν , $\nu \neq \mu$, we get the combined prior for α_μ

$$\mathcal{P}(\alpha_\mu) = \delta(\alpha_\mu) \sum_{r < r_\mu} \mathcal{P}(r) + p(\alpha_\mu) \sum_{r \geq r_\mu} \mathcal{P}(r). \quad (13)$$

By Eq. (10) the a priori means of all parameters are zero, and the variances are

$$\langle \delta \alpha_\mu^2 \rangle = \sigma_\mu^2 \sum_{r \geq r_\mu} \mathcal{P}(r). \quad (14)$$

Thus the bare variance σ_μ^2 is “renormalized” by the probability to be in a family, in which the parameter is nonzero. An interesting special case is

$$\mathcal{P}(r) \propto r^{-\gamma}, \quad \gamma > 1, \quad R \rightarrow \infty, \quad (15)$$

$$r_\mu = \mu. \quad (16)$$

³Nestedness, completeness, and normality of the prior are needed for comparison between nonparametric and parametric models discussed in later sections; in general, they are not required for Bayesian learning.

Then the a priori variance gets a simple form

$$\langle \delta \alpha_\mu^2 \rangle \propto \mu^{-\beta} \sum_{r=\mu}^{\infty} r^{-\gamma} \sim \mu^{-\beta-\gamma+1}. \quad (17)$$

Thus $\langle \delta \alpha_\mu^2 \rangle$ depends as much on the bare variance as on the speed of decay of $\mathcal{P}(r_\mu)$. This suggests that the learning properties of the nested setup will depend equivalently on both β and γ . However, the reality is not so simple.

Inference in our setup is done by means of the Bayes rule. The procedure is quite standard (Press, 1989; Bialek et al., 1996; Balasubramanian, 1997), and, for example, a posteriori expectations of parameter values are given by

$$\langle \alpha_\mu \rangle = \frac{\partial}{\partial J_\mu} \Big|_{\mathbf{J}=0} \log Z(\mathbf{J}), \quad (18)$$

$$Z(\mathbf{J}) \equiv \int d\boldsymbol{\alpha} \mathcal{P}(\boldsymbol{\alpha}) e^{-\mathcal{L}(\boldsymbol{\alpha}) + \mathbf{J} \cdot \boldsymbol{\alpha}} \quad (19)$$

$$= \sum_r \mathcal{P}(r) Z_r(\mathbf{J}), \quad (20)$$

$$Z_r(\mathbf{J}) \equiv \int d^{K(r)} \boldsymbol{\alpha} e^{-\mathcal{L}_r(\boldsymbol{\alpha}) + \sum_{\mu=1}^{K(r)} J_\mu \alpha_\mu}, \quad (21)$$

$$\mathcal{L}(\boldsymbol{\alpha}) \equiv \sum_{i=1}^N \phi(x_i | \boldsymbol{\alpha}), \quad (22)$$

$$\mathcal{L}_r(\boldsymbol{\alpha}) \equiv - \sum_{\mu=1}^{K(r)} \log p(\alpha_\mu) + \sum_{i=1}^N \phi(x_i | \boldsymbol{\alpha}), \quad (23)$$

$$\phi(x | \boldsymbol{\alpha}) \equiv - \log Q(x | \boldsymbol{\alpha}). \quad (24)$$

The posterior expectations are thus determined by the properties of the $Z(\mathbf{J})$, which can be calculated using the saddle point analysis for $N \gg 1$. This is difficult for the first form of $Z(\mathbf{J})$, Eq. (19), due to the singularity at $\alpha_\mu = 0$ [the singularity was also the reason why we left $\mathcal{P}(\boldsymbol{\alpha})$ out of the combined Lagrangian, Eq. (22)]. Hence we return to the nested form, Eq. (20, 21), but the equivalence between the representation should be kept in mind. Exchanging the order of integration and summation in Eqs. (19, 20) and similar is possible if the priors decay sufficiently fast at $r \rightarrow \infty$, or are regularized with regularization lifted after averages are calculated. Unless mentioned otherwise, this is always assumed.

The expectation of α_μ in the model families with $K(r) < \mu$ is necessarily zero, and a similar bias towards smaller magnitudes of parameters will be present when we average over families. Therefore, the a priori decrease of the variances with μ , Eqs. (14, 17), will persist a posteriori for finite N . This is the famous James and Stein (1961) shrinkage.

The saddle point, also called *classical* or *maximum likelihood*, values of parameters in each family, $\boldsymbol{\alpha}_r^* \equiv \{\alpha_{\mu;r}^*\}$, and the second derivatives matrix at the saddle, \mathbb{F}_r , are determined by (remember that $\alpha_{\mu;r}^* \equiv 0$ for $\mu > K(r)$)⁴

⁴The are possibilities of more than one saddle point and of other anomalies. This was analyzed by Bialek et al. (2001). The conditions to prevent such problems are mild, and we assume them to hold in what follows.

$$\left. \frac{\partial \mathcal{L}_r(\boldsymbol{\alpha})}{\partial \alpha_\mu} \right|_{\boldsymbol{\alpha}=\boldsymbol{\alpha}_r^*} = 0, \quad \mu \leq K(r), \quad (25)$$

$$\left. \frac{\partial^2 \mathcal{L}_r(\boldsymbol{\alpha})}{\partial \alpha_\mu \partial \alpha_\nu} \right|_{\boldsymbol{\alpha}=\boldsymbol{\alpha}_r^*} = \mathbb{F}_r^{\mu\nu}, \quad \mu, \nu \leq K(r). \quad (26)$$

To the first order in $1/N$, this gives

$$Z(\mathbf{J}) = \sum_r \mathcal{P}(r) \frac{\mathcal{P}(\boldsymbol{\alpha}_r^*|r)(2\pi)^{K(r)/2}}{N^{K(r)/2} \det^{1/2} \frac{\mathbb{F}_r}{N}} Q(\{x\}|\boldsymbol{\alpha}_r^*) e^{\frac{1}{2} \mathbf{J}_r \mathbb{F}_r^{-1} \mathbf{J}_r + \mathbf{J}_r \cdot \boldsymbol{\alpha}_r^*}, \quad (27)$$

where $\mu \leq K(r)$ components of \mathbf{J}_r are the same as those of \mathbf{J} , and all higher order components are zero. Differentiating, we get:

$$\langle \alpha_\mu \rangle = \frac{\sum_{r=1}^R \alpha_{\mu;r}^* e^{-\mathcal{L}(r)}}{\sum_{r=1}^R e^{-\mathcal{L}(r)}}, \quad (28)$$

$$\mathcal{L}(r) \equiv -\log \mathcal{P}(r) - \sum_{\mu=1}^{K(r)} \log p(\alpha_{\mu;r}^*) + \sum_{i=1}^N \phi(x_i|\boldsymbol{\alpha}_r^*) + \frac{K(r)}{2} \log \frac{N}{2\pi} + \text{Tr} \log \frac{\mathbb{F}_r}{N}. \quad (29)$$

For finite R , and $\beta = 0$, this is the usual Bayesian model family selection: a posteriori expectation of parameters is a weighted sum over posterior probabilities of families defined by $e^{-\mathcal{L}(r)}$. This posterior is not trivial: it includes the negative maximum likelihood term, $\sum_{i=1}^N \phi(x_i|\boldsymbol{\alpha}_r^*)$, which grows in magnitude linearly with N , but decreased as r grows due to nestedness. It also incorporates the fluctuation determinant $\frac{K(r)}{2} \log \frac{N}{2\pi} + \text{Tr} \log \frac{\mathbb{F}_r}{N}$, which grows only logarithmically in N , but increases with r . Depending on the value of N , there will be some r^* , for which $\mathcal{L}(r)$ is minimal. For large N , as a discrete analog of the saddle point argument, this value will dominate the sums in Eq. (28), hence some model family will be “selected.”

However, Eqs. (28, 29) become more interesting if one lets $R \rightarrow \infty$. The completeness condition ensures that for large enough r one will be overfitting the data, and $Q(x|\boldsymbol{\alpha}_r^*) \rightarrow 1/N \sum \delta(x - x_i)$. Therefore, if the sums are dominated by $r \rightarrow \infty$, then consistency breaks and the learning fails. One would thus expect two features of the setup to influence the success of the learning. First, it is the prior $\mathcal{P}(r)$, which switches on extra degrees of freedom: for slowly decaying priors one would expect $r \rightarrow \infty$ terms to win. Second, it is the dependence of the likelihood term on r , which measures how capable are the newly activated degrees of freedom of overfitting, or, equivalently, how fast $\max_i Q(x_i|\boldsymbol{\alpha}_r^*)$ grows.

From Eq. (29) it is easy to see that large r will have an exponentially small weight in the posterior probability if

$$\lim_{r \rightarrow \infty} \frac{N \max_i \log Q(x_i|\boldsymbol{\alpha}_r^*) + \log \mathcal{P}(r)}{K(r) \log N} = 0. \quad (30)$$

Under this condition $Q(x|\boldsymbol{\alpha}^*)$ will eventually approach the correct distribution, but not the sum of δ -functions. Colloquially, Eq. (30) requires the explanatory capacity of the new, high order degrees of freedom to be small enough so that keeping them always “on” does not make sense. This criterion is similar to the consistency condition of the Structural Risk

Minimization (SRM) theory, which requires that the Vapnik–Chervonenkis dimension, the SRM capacity measure of the selected model, grows slower than the number of samples to be explained (Vapnik, 1998; Nemenman, 2000).

As an example, let’s analyze how the condition in Eq. (30) may be violated for $K(r) \sim r$. In this case $\mathcal{P}(r)$ must be superexponential to be relevant for finding r^* . It is not required to decay at some minimal speed as might have been expected. Moreover, $\mathcal{P}(r)$ may actually grow subexponentially with r , forming a non-normalizable prior supported mostly at infinity.⁵ Due to light tails and small effective support, exponentially decaying priors are not very interesting, so we disregard the prior term in Eq. (30). Then, for a fixed large N , a finite r^* will be dominant if $\log Q(x_i|\alpha_r^*)/r \rightarrow 0$. That is, the growth of the δ function-like peaks of the maximum likelihood distribution should be superlinear in K , the number of parameters in the model family, in order for $r^* \rightarrow \infty$ and Bayesian setup to be inconsistent.

Finally, we remind the readers that, if each of $p(\alpha_\mu)$ has a noncompact support, or if the distance from $\bar{\alpha}$ to the boundary of A_r in the $K(r)$ -dimensional space is larger than ϵ , then the density of solutions for a K -parametric family is (Bialek et al., 2001)⁶

$$\rho(\epsilon; \bar{\alpha}) \approx \mathcal{P}(\bar{\alpha}|r) \frac{2\pi^{K/2}}{\Gamma(K/2)} \frac{\epsilon^{(K-2)/2}}{\sqrt{\det \mathcal{F}_K}}, \quad (31)$$

where

$$\mathcal{F}_K^{\mu\nu}(\bar{\alpha}) = \left. \frac{\partial^2 D_{\text{KL}}(\bar{\alpha}||\alpha)}{\partial \alpha_\mu \partial \alpha_\nu} \right|_{\alpha=\bar{\alpha}}. \quad (32)$$

$N\mathcal{F}_K$ is the Fisher information matrix (Cover and Thomas, 1991); its eigenvectors are the principal axes of the error ellipsoid in parameter space, and the (inverse) eigenvalues give the variances of parameter estimates along each of these directions. The prefactor $2\pi^{K/2}/\Gamma(K/2)$ is the area of the K -sphere. Equation (31) gives $\mathcal{D} \approx K/2 \log N$.

For each value of $\bar{\alpha}$ and r , we can find the model $\hat{\alpha}_r = \arg \min_{\alpha \in A_r} D_{\text{KL}}(\bar{\alpha}||\alpha)$, which best approximates $\bar{\alpha}$ in A_r , and define $D_r(\bar{\alpha}) \equiv D_{\text{KL}}(\bar{\alpha}||\hat{\alpha})$, the distance between $\bar{\alpha}$ and A_r . If $\bar{\alpha} \in A_r$, then $\bar{\alpha} = \hat{\alpha}$, and $D_r(\bar{\alpha}) = 0$. However, if $\bar{\alpha} \notin A_r$, then $D_r(\bar{\alpha}) > 0$ (cf. Fig. 1 for a sketch of these quantities). If the radius of curvature of A_r in the full $K(R)$ -dimensional space is much larger than ϵ , we get

$$\rho(\epsilon; \bar{\alpha}) = \sum_{r: D_r(\bar{\alpha}) \leq \epsilon} \mathcal{P}(r) \int d\alpha \mathcal{P}(\alpha|r) \delta[D_{\text{KL}}(\bar{\alpha}||\alpha) - \epsilon] \quad (33)$$

$$= \sum_{r: D_r(\bar{\alpha}) \leq \epsilon} \mathcal{P}(r) \mathcal{P}(\hat{\alpha}_r|r) \frac{2\pi^{K(r)/2}}{\Gamma[K(r)/2]} \frac{[\epsilon^2 - D_r^2(\bar{\alpha})]^{[K(r)-2]/4}}{\sqrt{\det \mathcal{F}_{K(r)}}}. \quad (34)$$

If the support of $p(\alpha_\mu)$ is (semi)compact, then the K -sphere surface area factor in the above formula is to be multiplied by the fraction of the sphere’s surface which falls into A_r .

⁵As mentioned above, we always need either a fast decay or a proper regularization of $\mathcal{P}(r)$ to be able to exchange the order of integrations and summations in arriving to Eq. (29).

⁶In reality, a different scaling dimension d_K may appear in these formulas instead of K , the number of free parameters. For example, for a redundant parameterization we may have $d_K < K$. Opposite situations, $d_K > K$ and even $d_K \rightarrow \infty$, are also possible.

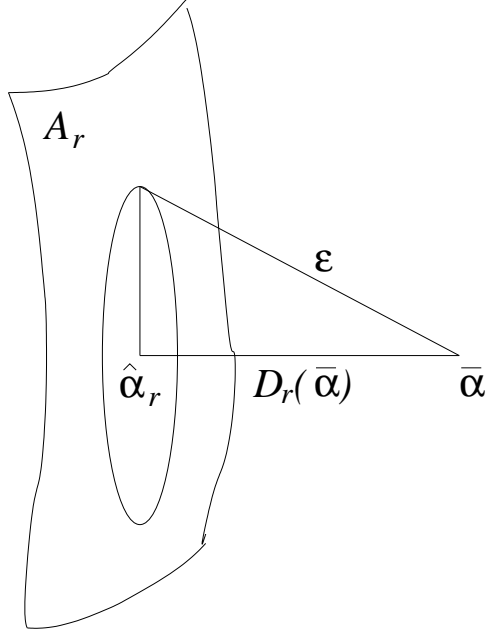


Figure 1: The target, its best estimate, and the ϵ -ball.

4 (Not quite) finite parameter learning: an example

As an example of the above construction, consider probability distributions on $[0, 1)$, with periodic boundary conditions, and with the logarithms of the distributions given by Fourier polynomials of degree r

$$\phi(x|\alpha) \equiv -\log Q(x|\alpha) = \alpha_0 + \sum_{\mu=1}^r (\alpha_{\mu}^{+} \cos 2\pi\mu x + \alpha_{\mu}^{-} \sin 2\pi\mu x), \quad (35)$$

$$\alpha_0 = \log \int dx \exp \left[-\sum_{\mu=1}^r (\alpha_{\mu}^{+} \cos 2\pi\mu x + \alpha_{\mu}^{-} \sin 2\pi\mu x) \right]. \quad (36)$$

The last equation is due to the normalization condition $\int dx Q(x|\alpha) = 1$, which sets $K(r) = 2r$, but not $2r + 1$ ⁷. With an appropriate choice of priors, Eqs. (8, 9), these families form a nested set, and the completeness for $R \rightarrow \infty$ follows from the Fourier theorem.

The classical solution for this parameterization is ($1 < \mu \leq r$)

$$\begin{aligned} \frac{\alpha_{\mu}^{*\pm}}{\sigma_{\mu}^2} + \sum_i \begin{pmatrix} \cos \\ \sin \end{pmatrix} 2\pi\mu x_i - N \int dx Q(x|\alpha^*) \begin{pmatrix} \cos \\ \sin \end{pmatrix} 2\pi\mu x \equiv \\ \frac{\alpha_{\mu}^{*\pm}}{\sigma_{\mu}^2} + \frac{N}{2} \Delta_{\mu}^{\pm} - \frac{N}{2} Q_{\mu}^{*\pm} = 0. \end{aligned} \quad (37)$$

⁷Instead of Eq. (36) one can treat α_0 as a dynamical variable and incorporate a δ -functional constraint $\delta[\alpha_0 - \alpha_0(\alpha^{\pm})]$ into the prior $\mathcal{P}(\alpha|r)$. This constraint can also be rewritten as $\delta[\int \exp[-\phi(x|\alpha)]dx - 1]$ to impose the normalization directly. This was the choice of Bialek et al. (1996).

Here Q_μ^\pm are the cosine (sine) amplitudes of the μ 'th mode in the Fourier expansion of $Q(x|\alpha)$, and Δ_μ^\pm are the same for the empirical probability density, $\sum \delta(x - x_i)$. Δ_μ^\pm are also the stochastic Fourier transform of $Q(x)$. The cosine–cosine components of the second derivative matrix at the saddle point are given by

$$\left. \frac{\partial^2 \mathcal{L}}{\partial \alpha_\mu^+ \partial \alpha_\nu^+} \right|_{\alpha=\alpha^*} = \frac{\delta_{\mu\nu}}{\sigma_\mu^2} + N \int dx Q(x|\alpha^*) \cos 2\pi\mu x \cos 2\pi\nu x - N \int dx Q(x|\alpha^*) \cos 2\pi\mu x \int dy Q(y|\alpha^*) \cos 2\pi\nu y \quad (38)$$

$$= \frac{\delta_{\mu\nu}}{\sigma_\mu^2} + \frac{N}{4}(Q_{\mu+\nu}^{*+} + Q_{\mu-\nu}^{*+}) + \frac{N}{2}Q_\mu^{*+}Q_\nu^{*+}, \quad (39)$$

and the sine–sine and the sine–cosine components are written similarly. This matrix is provably positive definite, thus for $N \rightarrow \infty$ we can perform the saddle point analysis.

For $\beta = 0$ the variance σ_μ^2 is constant, and we can neglect the first term in Eq. (37) in the limit of large N . This leads to the following solution of the saddle point equations:⁸

$$Q_\mu^{*\pm} \approx \Delta_\mu^\pm, \quad \mu = 1 \dots r. \quad (40)$$

For $\beta > 0$, $Q_\mu^{*\pm}$ will be corrected by a systematic β –dependent bias, which will tend to 0 for fixed μ as N grows. This will decrease the posterior variance of the estimator Q^* .

Equation (40) says that the first r pairs of coefficients $\alpha_\mu^{*\pm}$ are such that the corresponding Fourier amplitudes of the classical solution Q^* match those of the empirical one. By Nyquist theorem and the law of large numbers, for $r < N/2$, Δ_μ^\pm approach the Fourier amplitudes of the unknown target probability density \bar{Q} . Thus the low frequency modes will be learned well. However, if $r > N/2$ the saddle point solution will start to overfit and develop δ –like spikes at each observed data point. This is in accord with the observation we have already mentioned before: to guarantee consistency, the capacity of models, as measured by either the VC dimension or the scaling dimension of Bialek et al. (2001), which in this case is equal to the number of free parameters, must grow slower than N . It is instructive to observe this effect clearly in the model example.

These are the results for a fixed r . But what happens when we average over it? To avoid overfitting, we must make sure that the contribution of $r \rightarrow \infty$ to the posterior log–probability, Eq. (29), is negligible. In this regime, according to Eq. (40), the r available modes will create peaks of height $\sim r$ (remember the Fourier expansion of a δ –function) at the observed sample points. With $K(r) = 2r$ this ensures consistency by satisfying Eq. (30).

But we can go farther and prove that r^* is not only finite, but actually grows sublinearly in N , again paralleling results for SRM (Vapnik, 1998) and their Bayesian equivalent (Nemenman, 2000). Suppose $r \gg N$ dominates the posterior. Then, for a slowly decaying $\mathcal{P}(r)$, Eq. (29) can be rewritten as

$$\mathcal{L}(r) \sim -N \log r + r \log N, \quad (41)$$

⁸Equation (40) can be used as a basis of a numerical algorithm for estimating Q by putting a Dirichlet kernel $D_r(x) = 1 + 2 \sum_{\mu=1}^r \cos 2\pi\mu x = \frac{\sin((r+1/2)x)}{\sin x/2}$ at every sample point x_i , and then evaluating the posterior to estimate the best value of r . Such algorithm will be, at worst, quadratic in N and usually even faster. Use of other kernels with similar behavior near zero, such as the Fejer kernel, is also possible.

This is minimized (and the posterior probability is maximized) for $r^* \sim N/\log N$, and higher values of r are exponentially inhibited. This means that the assumption of $r \gg N$ being dominant is incorrect. Thus posterior probability is dominated by $r^* \lesssim N$ for all reasonable priors. This is, of course, the worst case estimation, and in many typical applications the value of r^* will be even lower, as we will see soon.

To better appreciate the importance of the fact that the nested learning setup is almost always consistent and the result of averaging over r is very weakly dependent on $\mathcal{P}(r)$, we have to contrast this to a seemingly very similar case of nonparametric learning.

5 (Not quite) nonparametric learning

Nonparametric learning usually refers to inferring a functional form of the probability density $Q(x)$ [or rather its negative logarithm, $\phi(x) \equiv -\log Q(x)$] with some smoothness constraints on it. The constraints may be in the form of explicitly bounding some derivatives of allowed Q or ϕ (possibly uniformly over all allowed functions), which was the choice of Hall and Hannan (1988) and Rissanen et al. (1992).⁹ Alternatively, in the Bayesian framework to be reviewed and developed here the constraints may be incorporated into a functional prior that makes sense as a continuous theory, independent of discretization of x on small scales. For x in one dimension, the minimal and the most common choice is (Bialek et al., 1996; Aida, 1999; Nemenman and Bialek, 2002)

$$\mathcal{P}[\phi(x)] = \frac{1}{\mathcal{Z}} \exp \left[-\frac{\ell^{2\eta-1}}{2} \int dx \left(\frac{\partial^\eta \phi}{\partial x^\eta} \right)^2 \right] \delta \left[\frac{1}{l_0} \int dx e^{-\phi(x)} - 1 \right], \quad (42)$$

where $\eta > 1/2$, \mathcal{Z} is the normalization constant, and the δ -function enforces normalization of Q . The hyperparameters ℓ and η are called the smoothness scale and the smoothness exponent, respectively. Fractional order derivatives are defined by multiplying by the wave number to the appropriate power in the Fourier representation of ϕ . Such a priori measure is equivalent to specifying a 1-dimensional Quantum Field Theory, and, correspondingly, QFT methods have been used to work out details of inference with this prior (Bialek et al., 1996; Holy, 1997; Nemenman and Bialek, 2002).

If, as usual, ϕ is periodic on $x \in [0, 1)$, then we can represent ϕ as a Fourier series, Eq. (35), with $r \rightarrow \infty$. Then, since the Jacobian of the transformation $\phi(x) \rightarrow \{\alpha_\mu^\pm\}$ is a constant, the prior, Eq. (42), amounts to Gaussian priors over the Fourier amplitudes with the variance given by (Nemenman and Bialek, 2002)

$$\langle (\delta\alpha_\mu^\pm)^2 \rangle = \frac{2}{\ell^{2\eta-1}} \frac{1}{(2\pi\mu)^{2\eta}}, \quad \mu > 0. \quad (43)$$

The a priori means of the amplitudes are, obviously, zero. The normalization constraint is equivalent to making α_0^+ non-dynamic and determined by $r \rightarrow \infty$ version of Eq. (36).

⁹These authors used histogramming density estimators. Such estimators have no apparent hierarchy of model families; this is especially true for Rissanen et al. (1992), who allowed locally varying bin widths. Thus these techniques can not be referred to as nested parametric methods. On the other hand, either of the estimators allows an arbitrarily precise fit to any probability density, and specifying the estimator requires, in principle, specifying an infinite number of break points and density values. This is the reason for treating the estimators as nonparametric, even though they produce estimates of a well defined functional form.

The system of coupled equations, Eq. (37), which described the saddle point for the parametric example, determines the saddle point in the nonparametric case as well, but now there are infinitely many such equations. We can use variational calculus to get an equivalent description in terms of a differential equation for the entire function $\phi(x)$

$$\ell^{2\eta-1} \mathbb{R}_{-2\eta} \frac{\partial^{2\eta} \phi^*(x)}{\partial x^{2\eta}} - N Q^*(x) + \sum_i \delta(x - x_i) = 0, \quad (44)$$

where $\phi^*(x)$ and $Q^*(x) \equiv \exp[-\phi^*(x)]$ are the saddle point values. The operator \mathbb{R}_θ shifts the phase of each Fourier component of its argument by $\pi\theta/2$ ¹⁰. As yet another connection with the finite parameter case, note that this differential equation can be written as a finite difference equation on a grid with the step size of δx . If we take $\delta x = 1/(2r)$, then this is equivalent to the Fourier representation of the density with r modes.

Bialek et al. (1996, 2001) have calculated the model density for $\epsilon \rightarrow 0$ and the fluctuation determinants for QFT models with various η . By noticing from Eq. (44) that N and ℓ can enter the solutions only in a combination $N/\ell^{2\eta-1}$, we can extend their results and recover correct dependencies not only on η , but also on ℓ :

$$\rho(\epsilon; \bar{\phi}) \approx A[\bar{\phi}] \epsilon^\xi \exp \left[-\frac{B[\bar{\phi}]}{\ell \epsilon^{1/(2\eta-1)}} \right] \quad (45)$$

$$\mathcal{D}(\bar{\phi}; N) \approx C[\bar{\phi}] \left(\frac{N}{\ell^{2\eta-1}} \right)^{1/2\eta}, \quad (46)$$

where A , B , and C are related functionals that do not depend on ℓ , and ξ depends only on η . For $\eta = 1$ all of these quantities have been explicitly calculated. In particular,

$$C[\bar{\phi}] \approx \frac{1}{2} \int dx \sqrt{\exp[-\bar{\phi}(x)]}. \quad (47)$$

From Eq. (45) the dependence of C on η can be easily calculated near $2\eta - 1 \rightarrow +0$,

$$C[\bar{\phi}] \sim (2\eta - 1)^{1/2\eta-1} \quad (48)$$

with an undetermined value at $2\eta = 1$. Here we remind the reader that as $\eta \rightarrow 1/2$, \mathcal{D} and I_{pred} become closer to being linear in N . As discussed by Bialek et al. (2001), problems with $\mathcal{D}(N)/N \rightarrow 1$ are the most complicated properly posed learning problems that exist.

We want to compare the nonparametric and the nested setups. Equations (17, 43) suggest that, at least at the level of the first two a priori moments, the cases are similar: the a priori means of the amplitudes are zero, and the variances fall off as power laws in the mode number. However, the field theory model requires the variance to decrease at least as fast as $1/\mu$ (remember that $\eta > 1/2$, otherwise ρ is identically zero at $\epsilon = 0$, and \mathcal{D} is formally (super)linear in N with the formally diverging prefactor, leading to diverging high frequency fluctuations), while the finite parameter case does not impose such constraints. Indeed, for $\beta = 0$ and $\gamma \rightarrow 1$ we may have $\langle (\delta\alpha^\pm)^2 \rangle$ as close to being a constant as we wish,

¹⁰For a comprehensive treatment of fractional differentiation the reader is referred to Samko et al. (1987). In particular, the action of the phase shift operator \mathbb{R}_θ may be calculated by the Wiener-Hopf method.

and, with a suitable regularization, $\langle(\delta\alpha^\pm)^2\rangle = \text{const}$ is possible. This is an indication of essential differences between the models: in the nested case, priors have a weaker influence on the consistency of learning.

How is the inconsistency manifested in the nonparametric case? From Eq. (44) we see that the derivatives of ϕ^* and Q^* of order $2\eta - 1$ have step discontinuities in them. Thus, for $2\eta = 1$ the classical solution itself, $\phi^*(x)$, will be discontinuous. For $2\eta < 1$ the singularities will be even more severe. We may characterize sample-dependent fluctuation in Q^* by Kullback–Leibler divergence, $D_{\text{KL}} = \int dx Q_1^*(x) \log Q_1^*(x)/Q_2^*(x)$ between Q_1 and Q_2 , the saddle point solutions for different realizations of the same size samples. If Q^* has, at least, step discontinuities at the sample points, and these points are random, then D_{KL} will not fall to zero as N increases, manifesting the inconsistency directly. Even though these problems develop for $\eta < 1/2$, the prior can still be properly normalized by either discretizing the space, or going to the Fourier representation. It is the possibility to overfit, not the improper Bayesian setup, which destroys learning¹¹. This is again in contrast to the finitely parameterized nested setup, where normalizable priors guarantee consistency.

In an attempt to remove sensitivity to priors in QFT learning, Bialek et al. (1996); Nemenman and Bialek (2002) treated ℓ as an unknown random variable (hyperparameter), introduced a prior for it, and averaged (similar averaging over η has not yet been performed). This is akin to nesting of finite dimensional models. Such setup is, indeed, consistent, and the integration “selects” the best value for ℓ and improves convergence for a wide range of target probability densities. On the other hand, integrating over ℓ produces the theory that is not necessarily local in $\phi(x)$ and couples all the Fourier amplitudes. It is difficult to compare such theory to the nested finite parameter setup directly. Therefore, we will not focus on averaging in what follows. Instead, we will assume that a priori values of η and ℓ used for learning are, indeed, the best for a particular target being learned.

6 Comparing the performance

So far the most important difference between the nested and the nonparametric setups is that the first seems to be very insensitive to the a priori variances of parameters (in the specific case, amplitudes of Fourier representation of the probability density being learned), while in the second this variance is crucial (at the moment we don’t consider averaging over ℓ or η). This distinction can be easily explained.

QFT nonparametric models do not have a sharp separation between the “active” and “passive” modes. While modes with low μ are determined by the data, the fluctuations of the amplitudes for larger μ are inhibited only due to their small a priori variances, Eq. (43), which fall off as power laws. The exact attenuation of the fluctuation depends on the detailed values of η and ℓ , and the cumulative contribution to posterior variance of the estimators may be substantial. In contrast, for the finite parameter nested case, once the most probable model family is determined, the higher order modes (and fluctuations caused by them) are inhibited *exponentially*. The cumulative fluctuations are then small and basically independent of the a priori variances of parameters, and the learning may succeed even

¹¹In the language of Quantum Field Theory, the tree level amplitudes remain well defined, but loop corrections lead to ultraviolet divergences.

for very slowly decaying (or not decaying at all) $\mathcal{P}(r)$.

Another set of differences can be seen when comparing the learning performance of the two setups. It is instructive to select two targets for testing. The first one is a distribution typical in Eq. (42). In accord with the comment made at the end of the previous Section, we choose the same fixed values of η and ℓ both for generating the target and for learning it. The second example has a finite number of Fourier modes, each with the same variance, and thus is typical in the nested case with β equal to zero and some a priori chosen γ .

When learning the first target by the QFT method, we will get from Eq. (46) $\mathcal{D} \propto (N/\ell^{2\eta-1})^{1/2\eta}$ and the expected universal learning curve is $\Lambda \propto 1/(N\ell)^{1-1/2\eta}$.¹² This asymptotics will kick in when $N \gg 1/\ell$. For smaller N , $\Lambda \sim 1$ and is barely decreasing. Now consider the nested model, Eqs. (35), which is “incorrect” for learning such distributions. It cannot perform better than the QFT prior, which is “correct” and, therefore, the best. The question is: how much worse the nested prior is?

We already know that r^* that minimizes Eq. (29) is much smaller than N . For r of this magnitude, the first r modes of the target are going to be well approximated by the estimate, and they will contribute $O(r/N)$ to the leading data dependent term in Eq. (29). The modes of the target above the r 'th won't be fitted by the estimate, and each of them contributes its variance of about $\ell^{-2\eta+1}\mu^{-2\eta}$ to the data dependent term, adding up to $\sum_{\mu=r+1}^{\infty} \ell^{-2\eta+1}\mu^{-2\eta} \propto (r\ell)^{-2\eta+1}$. Combined with the fluctuation determinant this gives

$$\mathcal{L}(r) \sim -N(r\ell)^{-2\eta+1} + r \log N \quad (49)$$

for determining the most probable r . Thus for $N \gg 1$ (in practice, when $\Lambda < 1$ in Eq. (52) below, that is for moderately large N)

$$r^* \propto \left(\frac{N}{\log N} \right)^{1/2\eta} \ell^{1/2\eta-1}, \text{ and} \quad (50)$$

$$\mathcal{D} \propto N^{1/2\eta} \left(\frac{\log N}{\ell} \right)^{1-1/2\eta}. \quad (51)$$

$$\Lambda \sim \left(\frac{\log N}{N\ell} \right)^{1-1/2\eta}. \quad (52)$$

It is difficult to trust the logarithmic terms in these expression since we've neglected the prior, some contributions to the data term, etc.¹³ In any case, in practice the logarithmic

¹²The prefactor in front of the fluctuation determinant and the learning curve may be very significant (and, possibly, diverging for especially ill-behaved targets). However, we will not analyze this here.

¹³If certain derivatives of the target distribution are known to satisfy some Lipschitz conditions then the Occam factor and the learning curve for histogramming density estimators provably have logarithmic contributions (Hall and Hannan, 1988; Rissanen et al., 1992). In contrast, prior to now, logarithmic corrections for QFT models, or for parametric learning of QFT-typical targets have not been analyzed. However, logarithmic differences between the cases were expected. The reason is quite clear. In discrete case with $\beta = 0$, once we know $K^* \sim N^\omega$, each parameter is free to vary with the same variance, giving the familiar $N^\omega \log N$ fluctuations. For the nonparametric case, $\sigma_\mu < \sigma_\nu$ for $\mu > \nu$. Thus each next parameter varies less, somewhat decreasing the total effective number of parameters. This was elucidated in detail by Bialek et al. (2001).

Such logarithmic difference between QFT and parametric setups have the same roots as the difference between cross-validation, bootstrap, and Akaike's model selection criterion on the one hand and Dawid's pre-

correction will be impossible to see since it will be masked by small N , statistical fluctuations both in the values of $\bar{\alpha}$ and x 's generated by them, and by the target-dependent prefactors in front of the universal scaling term. It is important, however, that the power law scaling is most definitely correct. It suggests immediately that the performance of the nested model is not much worse than that of the true one, if worse at all. In particular, the nested learning machine also can solve arbitrarily complex inference problems.

A rigorous way to estimate performance of the nested learning on a nonparametric target is to calculate the integral $\langle \rho(\epsilon) \rangle = \int d\bar{\alpha} \mathcal{P}(\bar{\alpha}) \rho(\epsilon; \bar{\alpha})$, where ρ is of the form Eq. (34), and the averaging is done over the QFT prior, and then calculate \mathcal{D} and Λ from this averaged ρ . This is difficult, and instead we may choose to replace $\langle \rho(\epsilon) \rangle$ by $\rho(\epsilon; \bar{\alpha}_{\text{typ}})$, where $\bar{\alpha}_{\text{typ}}$ is a typical target in the nonparametric prior, Eq. (42).¹⁴ For such $\bar{\alpha}_{\text{typ}}$, $D_r(\bar{\alpha}) \sim \sum_{\mu > r} \ell^{-2\eta+1} \mu^{-2\eta} \propto (\ell r)^{-2\eta+1}$. Further, $\mathcal{P}(\hat{\alpha}_{\mu; \text{typ}}^\pm | r) \sim \exp[-0.5 \mu^{-2\eta} \ell^{-2\eta+1} / \sigma_\mu^2]$. In our case, $\sigma_\mu^2 \sim \mu^{-2\beta}$. Therefore, for $2(\eta - \beta) > 1$, which is satisfied for $\eta > 1/2$ and $\beta = 0$, this gives $\mathcal{P}(\hat{\alpha}_r | r) \sim \exp[-\sum_{\mu=1}^r \mu^{-2\eta} \ell^{-2\eta+1} / \sigma_\mu^2] \sim \exp[C_1 - C_2 r^{-2(\eta-\beta)+1}]$, where C_1 and C_2 are constants. For large enough r , this whole expression tends to a constant. Thus, combining with Eq. (34), we get

$$\rho(\epsilon; \bar{\alpha}_{\text{typ}}) \sim \sum_{r: r^{-2\eta+1} \leq \epsilon} \mathcal{P}(r) \frac{2\pi^r}{\Gamma(r)} \frac{[\epsilon^2 - (\ell r)^{-4\eta+2}]^{(r-1)/2}}{\sqrt{\det \mathcal{F}_{K(r)}}}. \quad (53)$$

If $\mathcal{P}(r)$ is subexponential as before, we can get the scaling of ρ to the leading order in small ϵ by calculating the sum in Eq. (53) using the saddle point analysis and taking just the zeroth order (saddle point) term. The saddle value for r is $r^* \sim \epsilon^{-1/(2\eta-1)} \ell^{-1}$, which gives

$$\rho(\epsilon; \bar{\alpha}_{\text{typical}}) \sim \epsilon^{\epsilon^{-1/(2\eta-1)} \ell^{-1}}, \quad (54)$$

with the first subleading term of $O(\exp[-\epsilon^{-1/(2\eta-1)} \ell^{-1}])$. Doing the same leading order saddle point evaluation of the integral in Eq. (2), we now get $\epsilon^* \sim (N\ell / \log N)^{1/2\eta-1}$, which again results in Eq. (51).

In summary, learning a distribution typical in the nonparametric model by means of the nested setup results in a possible logarithmic performance loss. What if instead we study a distribution that is typical in the nested case? For $\beta = 0$, this will be a distribution with \bar{r} modes, where \bar{r} is determined according to $\mathcal{P}(\bar{r})$, and each of the active modes will have an amplitude $\sim \sigma$. For $N \lesssim \bar{r}$, no learning machine will be able to estimate $2\bar{r}$ amplitudes, so Λ will be almost flat and will not have a well defined scaling (Nemenman and Bialek, 2002). The differences between learning machines emerge for $N \gg \bar{r}$.

In the nested setup, to calculate the density of states we need to know $D_r(\bar{\alpha})$. But this is either exactly zero (for $r \geq \bar{r}$), or large (for $r < \bar{r}$) since for $\beta = 0$ typically each of the quential statistics and Bayesian model selection on the other (Stone, 1977; Dawid, 1984). There too the difference in estimating the magnitude of prediction error comes from the fact that most of the parameters active at given N have been latent for smaller sample sizes.

¹⁴Much of this paper is about Bayesian model selection, which chooses an appropriate model as a balance between a good fit and a high complexity. Similarly, we have to ask if the complexity of calculating $\langle \rho(\epsilon) \rangle$ is worth the benefit this quantity will provide over $\rho(\epsilon; \bar{\alpha}_{\text{typ}})$, which is knowing the prefactors in \mathcal{D} and Λ exactly. As I don't believe that any of the priors studied in this work will be *exactly* realized in nature, knowing the prefactors is, therefore, not a priority.

target amplitudes is large. So Eq. (34) transforms to

$$\rho(\epsilon; \bar{\alpha}_{\text{typ}; \bar{r}}) \sim \sum_{r \geq \bar{r}} \mathcal{P}(r) \mathcal{P}(\hat{\alpha}_r | r) \frac{2\pi^r}{\Gamma(r)} \frac{\epsilon^{r-1}}{\sqrt{\det \mathcal{F}_K}}, \quad (55)$$

where $\bar{\alpha}_{\text{typ}; \bar{r}}$ is a distribution typical in A_r . This is dominated by $r = \bar{r}$, and the other terms are negligible for $\epsilon \rightarrow 0$. Thus asymptotically the performance of the nested learning machine will differ from that of the a priori correct parametric one only by the prefactor $\mathcal{P}(r)$. However, this enters only logarithmically in the expression for \mathcal{D} and is negligible for a slowly decreasing $\mathcal{P}(r)$. Therefore, the learning curve is

$$\Lambda(N) = \begin{cases} \sim 1, & N < \bar{r}, \\ \frac{\bar{r}}{2N}, & N > \bar{r}. \end{cases} \quad (56)$$

We can now average over $\mathcal{P}(\bar{r})$, but this is not very informative.

The QFT setup will perform very differently with such target. For small N it will start similarly to Eq. (56). However, when $\Lambda \rightarrow 0$ and all \bar{r} modes are well approximated, the machine will continue trying to fit higher order modes, which it expects to be present even though they are not. This will result in the same fluctuation determinant as in Eq. (46), switching to the usual asymptotic $\Lambda \propto (N\ell)^{1/2\eta-1}$ instead of \bar{r}/N as in Eq. (56). Averaging over ℓ may help [in particular, for $\eta = 1$ the asymptotic scaling changes to $N^{-2/3}$ (Nemenman and Bialek, 2002)], but recovery will not be complete. It is possible that averaging over η can produce even better improvements, but this is yet to be analyzed.

So, when the target has finite number of degrees of freedom, the nested setup is qualitatively faster than the QFT learning machine!

7 Determining the underlying model: Trailing a changing target

One never needs to know the distribution that generated the data to an infinite precision, and some $\epsilon > 0$ approximation is enough. Further, if learning in biological systems is realized by *stochastic* gradient descent, as is argued, for example, by Seung (2003), then ϵ is bounded from below by the noise variance. As shown by Fairhall et al. (2002) and especially by Gallistel et al. (2001), convergence to the “good enough” estimate happens so quickly, that the transient learning curves are difficult to resolve. Is then the performance difference between the nested and the QFT scenarios seen in the previous section important? And, if yes, how can we observe it experimentally?

The answer may come from noticing that often the target itself changes while being learned. An ambient light intensity may be fluctuating while our eye estimates it, or the variance of angular velocities measured by a fly motion sensitive neuron can be varied by an experimenter while the fly tries to adapt to it, as was the case in the experiment by Fairhall et al. (2002). In these cases one has to learn constantly to stay at the allowed ϵ -error, and then a faster learning machine may be truly advantageous. However, even for a variable target, the nested learner will not be helpful if (a) a small change of the target parameters throws it back to a very large Λ , or (b) the changing target may drift to a region where \bar{r} is so large that the nested setup is not better than the nonparametric anymore.

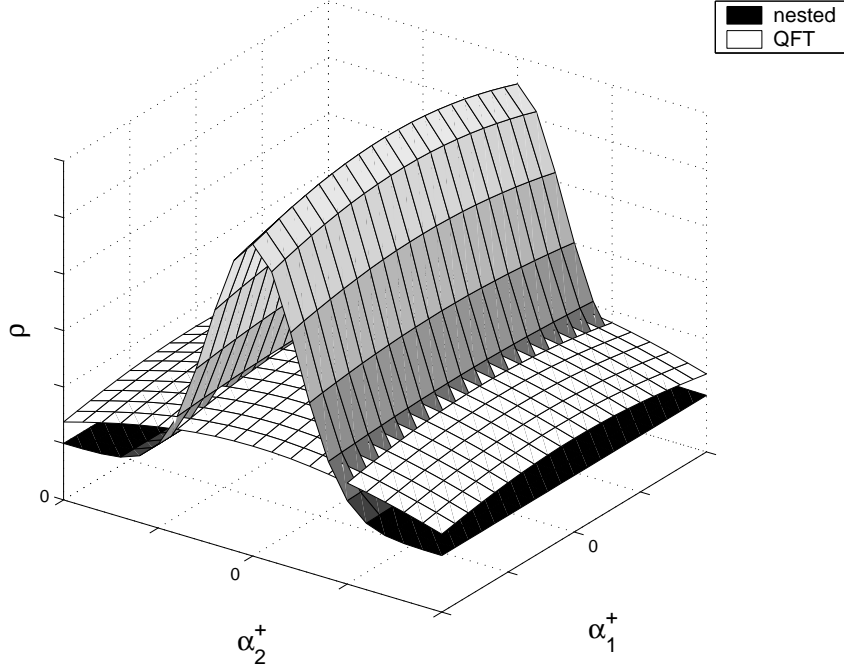


Figure 2: Schematic density of models as a function of the target location.

To answer these concerns, instead of focusing on the density of solutions as a function of the allowed error ϵ , we will keep ϵ fixed and vary $\bar{\alpha}$. For some small ϵ , a schematic drawing of dependence of ρ on $\bar{\alpha}_1^+$ and $\bar{\alpha}_2^+$ with the other parameters fixed at 0 is shown on Fig. 2. Since ϵ independent prefactors in Eq. (45) depend on the target very weakly, ρ in the QFT case is almost uniform. In the nested case, there is a ridge along $\alpha_2^+ \approx 0$, where the density is, at least, $\sim 1/\sqrt{\epsilon}$ larger than anywhere else, cf. Eq. (34). The ridge comes from the prior, Eq. (12), for $\alpha_2^+ = 0$ being singularly higher than for $\alpha_2^+ \neq 0$, and the singularity is then smoothed out by ϵ -approximation. In comparison, the nonparametric prior has a smooth bivariate normal shape, which does not survive ϵ -smearing and contributions from the higher order harmonics to the density.¹⁵

Figure 2 answers both of the concerns mentioned above. For a QFT machine, densities are everywhere small. So a small change of the target means vast and slow relearning. In contrast, if for a nested case $\bar{\alpha}$ is in the “large density” region, then there are many other models in the vicinity, and small changes of the parameters will likely leave the target close, so that not much will need to be relearned. Further, since the ridge drops off smoothly, models in the vicinity of a large density target also have large densities, and thus are fast to learn themselves. This will, of course, hold only when there is the most variable

¹⁵The plots of $\mathcal{P}(\bar{\alpha})$ and $\rho(\epsilon; \bar{\alpha})$ have very different meanings. The volume under the $\mathcal{P}(\bar{\alpha})$ surface is fixed by the normalization condition $\int d\bar{\alpha} \mathcal{P}(\bar{\alpha}) = 1$. Thus high a priori probability on any singular line, such as $\alpha_2^+ = 0$, necessarily means lower prior elsewhere. Such considerations are the reason for many so called *no free lunch* theorems [cf. Wolpert (1995)]. In the language of the density of solutions, the normalization condition can be rewritten as $\int d\epsilon \rho(\bar{\alpha}; \epsilon) = 1$. However, there are no constraints on the density integrated over $\bar{\alpha}$, and large density for some targets does not necessarily result in lower density elsewhere.

target direction, and the ridge is aligned with it. Importantly, since at a finite ϵ the ridge has a finite width, a perfect alignment is *not necessary*! This crucial observation together with our discussion of natural signals in the Introduction says that we can reasonably hope to find natural systems with ridges *approximately* adjusted to the fast variance directions.

Let's now analyze a few toy examples of variable targets and of their learning by different learning machines.¹⁶ We denote by $\hat{\alpha}$ an estimate of $\bar{\alpha}$ averaged over many presentations of the same data. We keep all but one parameter fixed (or changing very slowly), while $\bar{\alpha}_1(t)$, which is approximately the direction of the ridge in the density of solutions, is allowed to vary. If data are observed for a long time, then $\bar{\alpha}_\mu \approx \hat{\alpha}_\mu$ for all μ but 1. Now remember that Λ is the expected Kullback–Leibler divergence between $\bar{\alpha}$ and $\hat{\alpha}$, which converges to the χ^2 distance when it is small. Thus if $\bar{\alpha}_1 - \hat{\alpha}_1$ is not large,

$$\Lambda \propto (\hat{\alpha}_1 - \bar{\alpha}_1)^2. \quad (57)$$

For fixed target, when the learning curve is small and reaches its asymptotic scaling,

$$\frac{\partial \Lambda}{\partial N} = -\zeta_N \Lambda^\nu. \quad (58)$$

Here, in particular, $\nu = 1$ corresponds to a finite set of solutions along the direction of α_1 , $\nu = 2$ is the finite-parameter or nested case, and $\nu = 3$ is the $\eta = 1$ QFT model. In principle, other values of $\nu \in (0; \infty)$ are possible, though it is difficult to imagine which processes could lead to some of them. The constant $\zeta_N \sim 1$ depends on the details of the learning setup. For parametric cases, $\zeta_N = 2/K(\bar{r})$, and it can be calculated for other learning machines as well.

Can Eq. (58) be true for a variable target, or will the past experience, the inertia of previous observations, keep the estimate far from $\bar{\alpha}$? For Eq. (58) to hold, the learning machine must quickly notice the target variation and disregard old incorrect data. Gallistel et al. (2001) show that a rat reacts to changes in the reward rates as fast an ideal detector would. Therefore, the assumption is reasonable for biological systems.¹⁷

If measurements are taken at a fixed rate, so that $dN/dt = \text{const}$, we can combine Eq. (57) with the differential equations for Λ to get

$$\frac{d\Delta}{dt} = -\zeta \text{sign}(\Delta) |\Delta|^{2\nu-1} - v_{\bar{\alpha}}, \quad (59)$$

where $\Delta = \hat{\alpha}_1 - \bar{\alpha}_1$ is the average error of the estimation, ζ is some unknown constant with the dimensionality of $1/t$ and is basically the (adjusted) sampling rate, and $v_{\bar{\alpha}}$ is the drift velocity of the target. Let's consider a few different examples of $v_{\bar{\alpha}}$.

If $v_{\bar{\alpha}} = \mathcal{A}$ is a constant, then asymptotically for $t \rightarrow \infty$, setting $d\Delta/dt = 0$, we find

$$\Delta \rightarrow \Delta_\infty = - \left(\frac{\mathcal{A}}{\zeta} \right)^{1/(2\nu-1)}. \quad (60)$$

¹⁶I am unfamiliar with any comprehensive treatment of variable targets. Some interesting work was done by DeWeese and Zador (1998), and, properly adapted, the ideas of Atwal and Bialek (2004) are also useful.

¹⁷Here we leave aside important comments due to DeWeese and Zador (1998), who argued that time needed to notice the change of a target may be not invariant with respect to the direction of the change. Also note that for the nonparametric setup it takes longer to see that the target is changing. Thus the memory effects are more pronounced in this case, making our subsequent estimates of performance differences between the QFT and the nested learning conservative.

The ratio $v_{\bar{\alpha}}/\zeta$ must be $\ll 1$, otherwise Δ is outside of the $\Lambda \rightarrow 0$ asymptotic, for which Eq. (58) is valid. Thus, for small drifts, setups with smaller ν win qualitatively.

It is also of interest to consider the situation when $\bar{\alpha}_1$ undergoes a Brownian motion, $\langle v_{\bar{\alpha}}(t)v_{\bar{\alpha}}(t') \rangle = \Omega \delta(t-t')$. Writing the Fokker-Planck equation for this Langevin dynamics, we easily find the stationary distribution of Δ ,

$$P(\Delta) = \frac{\nu}{\Gamma\left(\frac{1}{2\nu}\right)} \left(\frac{\zeta}{\nu\Omega}\right)^{1/(2\nu)} \exp\left\{-\frac{\zeta|\Delta|^{2\nu}}{\nu\Omega}\right\}, \quad (61)$$

which results in the rms fluctuations of

$$\Delta_{\text{rms}} = \left\{ \nu^{1/\nu} \frac{\Gamma\left(\frac{3}{2\nu}\right)}{\Gamma\left(\frac{1}{2\nu}\right)} \right\}^{1/2} \left(\frac{\Omega}{\zeta}\right)^{1/(2\nu)}. \quad (62)$$

Again, these results are true only if $\Delta_{\text{rms}} \ll 1$, and again smaller ν provides for better trailing of the target.

Finally, inspired by Fairhall et al. (2002), let's examine the case of a periodic motion of $\bar{\alpha}_1$ and take, for simplicity, $\bar{\alpha}_1 = \mathcal{A} \sin \omega t$, and $v_{\bar{\alpha}} = \mathcal{A}\omega \cos \omega t$. Now Eq. (59) does not have a simple solution. However, we search for an asymptotically periodic $\Delta(t)$ with the same angular frequency of ω . Therefore, if we multiply Eq. (59) by $\cos \omega t$, integrate over a full period, and exchange the order of the differentiation and the integration, we get

$$\frac{d\langle \Delta \cos \omega t \rangle}{dt} = -\zeta \langle \text{sign}(\Delta) |\Delta|^{2\nu-1} \cos \omega t \rangle - \mathcal{A}\omega \langle \cos^2 \omega t \rangle, \quad (63)$$

where $\langle \dots \rangle$ denotes averaging over the period. Since we are looking for stationary oscillations, time derivative applied to any average is zero. This gives

$$\langle \text{sign}(\Delta) |\Delta|^{2\nu-1} \cos \omega t \rangle = -\frac{\mathcal{A}\omega}{2\zeta}. \quad (64)$$

Now multiplying Eq. (59) by $\text{sign}(\Delta) \Delta^{2\nu-1}$ and averaging again results in

$$\langle |\Delta|^{4\nu-2} \rangle = \frac{(\mathcal{A}\omega)^2}{2\zeta^2}, \quad (65)$$

which is the same scaling as in Eq. (60). However, now we also have dependence on ω .

There are other interesting cases yet to be analyzed, such as a step jump in the target, $\bar{\alpha}_1$, its square wave modulation, or its continuous bounded diffusion with short correlation time (Ornstein-Uhlenbeck process). Interestingly, the last two of these cases were used experimentally by Fairhall et al. (2002). However, we will leave the analysis for the future, when it will answer some specific question and won't be just a mathematical exercise. Even with the three examples already discussed, it is clear that, if the target is expected to move, the nested parametric setup will be able to trail it much closer than the nonparametric one, and the dependence on the amplitude of the motion is very different.

8 Discussion

The learning–theoretic ramifications of the above analysis are quite clear: the nested setup may learn much faster than the QFT one. Thus if one desires a complete learning machine, and there is no specific a priori reason to do the opposite (such as, knowing that the world is unlikely to have sharp cutoffs), a nested machine should be built. The differences are especially obvious when the target is allowed to vary along a large density dimension of the nested prior.

Instead of discussing this further, let us focus on possible biological applications. As mentioned in the Introduction, one is often faced with the questions like: Is the performance of the organism in learning a signal optimal? What is the equivalent learning–theoretic description of the computation done by it? These questions are usually asked in the situations when the natural signals, to which the organisms are adjusted in the course of the evolution, have only a few “important”, fast varying dimensions.

We have analyzed the best asymptotic learning rates under such conditions. Barely observable transients in the learning curves result in different scaling dependence of the estimation errors on the amplitude of the target’s motion. These effects are *stationary* and should be much easier to observe! The experimenter will have to deal with small target velocities, so that the asymptotic analysis presented here is valid, and the arguments of DeWeese and Zador (1998) do not apply (it might be better to leave variances aside altogether and study learning of other parameters). In addition, one will have to be careful to disentangle learning the input from adapting to it [as an example, a fly learns that the variance of the input signal has changed and rescales the input/output relation very fast, but the adaptation of the firing rate may take a lot longer (Fairhall et al., 2002)]. However, it is possible that these and other disadvantages will be outweighed by the ability to determine the correct learning–theoretic model of the organism’s inference process by varying the amplitude and the nature (say, from stochastic to periodic) of the target’s motion and studying the typical estimation error as a function of these parameters.

Consider, for example, the experiment described on Fig. 4 of Fairhall et al. (2002). There the input signal (the standard deviation of the angular velocity, $\sigma(t)$) undergoes a finite variance Σ^2 and a finite correlation time τ random motion. The instantaneous neuron firing rate $r(t)$ is the estimate of $\sigma(t)$. Repeating exactly the same randomly generated stimulus many times and averaging over spike trains, one may estimate $r(t)$ and, consequently, the rms estimation error $\Delta_{\text{rms}} = \langle (\sigma(t) - r(t))^2 \rangle_t^{1/2}$. Studying dependence of Δ_{rms} on Σ and τ along the lines of Eq. (62), one can estimate ν . Any $\nu \neq 2$ uniquely determines the underlying computational model. For $\nu = 2$, to distinguish a usual finite parameter model from the one that is nested, one makes the signal multidimensional (other parameters of the angular velocity, such as the mean and the skewness, vary together with σ). For, at least, some signal extensions, the nested model will change the magnitude (but not the scaling) of Δ_{rms} since $\zeta \propto 1/K(\bar{r})$. In contrast, the simpler model will keep the same prefactors and may stop converging close to the target altogether. Such analysis should lead to better understanding of the fly motion detection system.

In cognitive experiments of Gallistel et al. (2001) a rat was trying to learn rates of different rewards and *match* its foraging habits correspondingly. The rat’s ability to detect rate changes was (favorably) compared to a certain “ideal” Bayesian change detector, which

assumed not more than one such change during an experiment, and whose decisions were uninfluenced by the frequency of rate changes in the immediate past. Both of these assumptions are questionable in view of the experimental data presented in that paper. But which other model of the rat's behavior should be used instead? Just like in the fly case, one can vary the reward rates continuously, repeat experiments many times, and then look at the average mismatch between the stimulus and the response. Randomly fluctuating rates are preferred to exclude the possibility of the animal learning their functional form. Then dependence of the mismatch on the correlation time and the variance of the rates will point at a proper class of learning-theoretic models to compare the rat to.

Similarly, one can study the size of hysteresis effects, common in psychological experiments, as a function of the speed and the amplitude of the changes in stimuli, and this will act as a useful indicator of the type of machinery implemented by the brain. Or one can do this type of analysis on artificial neural networks designed explicitly to model particular animal behavior (Seung, 2003); this will build connections between network architectures and types of inference tasks performed by them.

Let us note another plausible, but clearly far fetched, application. Many researchers are interested in studying changes of susceptibility to learning with age [a famous example is by Knudsen (2002)]. Generally, a young subject can learn many things that an adult cannot. While such differences are usually attributed to physiological changes of (synaptic) plasticity with age, it would be nice to explain them partially as learning-theoretic consequences of long duration and small variability of the inputs.¹⁸ Hand waving arguments suggest that the explanation may lie in the collapse of the priors. That is, if one never observes a particular event, the expectation to see it in the future drops. Once it actually happens, one is then unable to discern it from the outcomes that have higher a priori probabilities. Our results suggest another route, where collapsing priors are actually advantageous. Having very little detailed knowledge of its environment early in life, an animal may be born with a simple QFT-like prior, which embodies the least expectations and does not have strongly preferred high variance dimensions. The environment, however, does. If a young animal is exposed to the variance immediately, it may collapse its very general prior into a nested structure roughly aligned with the most variable environmental dimensions, facilitating faster learning in the future. If such exposure does not happen till an older age, the animal will be forced to use uncollapsed QFT priors for learning, which, as we know now, may be detrimental to its success for certain simple, finite parameter problems.

Finally, let us finish with the following questions. Neuronal and neural networks are usually drawn as homogeneous, layered, and often self-similar objects. They are also believed to be fairly general computational machines, able to solve the most diverse problems. On the other hand, topology of biochemical and genetic networks is seemingly very irregular and modular.¹⁹ Their environment, while also diverse, usually varies in a simpler way. Can it be that the brain implements a nonparametric machine, while the other networks prefer the nested scenario, and the difference of the topologies is a manifestation of the chosen designs? Or maybe the nested models realize the idea of Minsky (1961) that,

¹⁸If such explanation is possible, it gives some hope that the inability to learn new things, which we all experience with age, is at least somewhat reversible.

¹⁹See, for example, <http://ecocyc.org:1555/ECOLI/new-image?type=OVERVIEW> for a schematic diagram of the *E-coli* metabolic pathways.

to learn arbitrary complex goals, one must decompose them into simpler ones?

Acknowledgments

I thank William Bialek and Chris Wiggins for many stimulating discussions. I am also grateful to Ila Fiete for carefully reading this manuscript and providing important feedback. This work was supported by NSF grant PHY99-07949 to Kavli Institute for Theoretical Physics and in part by NSF grant ECS-0332479 to Chris Wiggins and myself.

References

- T Aida. Field theoretical analysis of on-line learning of probability distributions. *Phys. Rev. Lett.*, 83:3554–3557, 1999.
- J Atick. Could information theory provide an ecological theory of sensory processing? In W Bialek, editor, *Princeton Lectures on Biophysics*, pages 223–289. World Scientific, Singapore, 1992.
- F Attneave. Some informational aspects of visual perception. *Psych. Rev.*, 61, 1954.
- G Atwal and W Bialek. Ambiguous model learning made unambiguous with $1/f$ priors. In S Thrun, L Saul, and B Scholkopf, editors, *Adv. Neur. Inf. Proc. Syst.*, volume 16. MIT Press, Cambridge, MA, 2004.
- V Balasubramanian. Statistical inference, Occam’s razor, and statistical mechanics on the space of probability distributions. *Neur. Comp.*, 9:349–368, 1997.
- H Barlow. Sensory mechanisms, the reduction of redundancy and intelligence. In D Blake and A Uttley, editors, *Proc. Symp. Mechanization of Thought Processes*, volume 2, pages 537–574. H M Stationery Office, London, 1959.
- H Barlow. Possible principles underlying the transformation of sensory messages. In W Rosenblith, editor, *Sensory Communication*, pages 217–234. MIT Press, 1961.
- W Bialek, C Callan, and S Strong. Field theories for learning probability distributions. *Phys. Rev. Lett.*, 77:4693–4697, 1996.
- W Bialek, I Nemenman, and N Tishby. Predictability, complexity, and learning. *Neur. Comp.*, 13:2409–2463, 2001.
- B Clarke and A Barron. Information-theoretic asymptotics of Bayes methods. *IEEE Trans. Inf. Thy.*, 36:453–471, 1990.
- T Cover and J Thomas. *Elements of Information Theory*. John Wiley & Sons, New York, 1991.
- F Cucker and S Smale. On the mathematical foundations of learning. *Bull. (New Series) of the Amer. Math. Soc.*, 39(1):1–49, 2001.

- AP Dawid. Present position and potential developments: some personal views. Statistical theory: the prequential approach. *J. Roy. Stat. Soc. A*, 147 (part2):278–292, 1984.
- P Detwiler, S Ramanathan, A Sengupta, and B Shraiman. Engineering aspects of enzymatic signal transduction: Photoreceptors in the retina. *Biophys. J.*, 79:2801–2817, December 2000.
- M DeWeese and A Zador. Asymmetric dynamics in optimal variance adaptation. *Neur. Comp.*, 10:1179–1202, 1998.
- A Fairhall, G Lewen, W Bialek, and R de Ruyter van Steveninck. Efficiency and ambiguity in an adaptive neural code. *Nature*, 412:787–792, 2002.
- CR Gallistel, T Mark, AP King, and P Latham. The rat approximates an ideal detector of changes in rates of reward: Implications for the law of effect. *J. Exper. Psych.: Animal Behav. Proc.*, 27:354–372, 2001.
- P Hall and EJ Hannan. On stochastic complexity and nonparametric density estimation. *Biometrika*, 75(4):705–714, 1988.
- T Holy. Analysis of data from continuous probability distributions. *Phys. Rev. Lett.*, 79: 3545–3548, 1997.
- W James and C Stein. Estimation with quadratic loss. In J Neyman, editor, *Proc. Fourth Berkeley Symposium Mathematical Statistics and Probability*, volume 1, pages 361–379, Berkeley, CA, 1961. University of California Press.
- ET Janes. Inference, method, and decision: Towards a Bayesian philosophy of science. *J. Amer. Stat. Assoc.*, 74(367):740–741, 1979.
- H Jeffreys. Further significance tests. *Proc. Camb. Phil. Soc*, 32:416–445, 1936.
- E Knudsen. Instructed learning in the auditory localization pathway of the barn owl. *Nature*, 417:322–328, 2002.
- D MacKay. Bayesian interpolation. *Neur. Comp.*, 4:415–448, 1992.
- M Minsky. Steps toward artificial intelligence. *Proc. IRE*, 49:8–30, 1961.
- I Nemenman. *Information Theory and Learning: A Physical Approach*. PhD thesis, Princeton University, Department of Physics, 2000.
- I Nemenman and W Bialek. Occam factors and model-independent bayesian learning of continuous distributions. *Phys. Rev. E*, 65:026137, 2002.
- SJ Press. *Bayesian statistics: principles, models, and applications*. John Wiley & Sons, New York, 1989.
- Rajesh P. N. Rao. Bayesian computation in recurrent neural circuits. *Neur. Comp.*, 16(1): 1–38, 2004.

- J Rissanen. *Stochastic Complexity and Statistical Inquiry*. World Scientific, Singapore, 1989.
- J Rissanen, T Speed, and B Yu. Density estimation by stochastic complexity. *IEEE Trans. Inf. Thy.*, 38(2):315–323, 1992.
- S Samko, A Kilbas, and O Marichev. *Integraly i proizvodnye drobnogo poriadka i nekotorye ikh prilozheniia*. Nauka i tekhnika, Minsk, Belarus, 1987. In Russian.
- G Schwartz. Estimating the dimension of a model. *Ann. Stat.*, 6:461–464, 1978.
- HS Seung. Learning in spiking neural networks by reinforcement of stochastic synaptic transmission. *Neuron*, 40:1063–1073, 2003.
- M Stone. An asymptotic equivalence of choice of model by cross-validation and Akaike’s criterion. *J. Roy. Stat. Soc. B*, 39(1):44–47, 1977.
- V Vapnik. *Statistical Learning Theory*. John Wiley & Sons, New York, 1998.
- D Wolpert. On the Bayesian “Occam factors” argument for Occam’s razor. In T Petsche et al., editors, *Computational Learning and Natural Learning Systems*, volume 3. MIT Press, 1995.